Advanced Ceramics Progress: Vol. 11, No. 2, (Spring 2025) 42-49

Materials and Energy Research Center
MERC

Contents lists available at ACERP

Advanced Ceramics Progress

Journal Homepage: www.acerp.ir

Original Research Article

Mechanical and Tribological Properties of Ti-6Al-4V by Deposition of Multilayered Coating with PACVD Technique

Ali Newpour [a], Milad Kazemi [b], Masoud Rajabi [c]*, Hamed Ghorbani [d]

[a] *MSc Candidate, Department of Materials Science & Engineering, Faculty of Technology and Engineering, Imam Khomeini International University (IKIU), Qazvin, Iran.*
[b] *MSc Candidate, School of Metallurgy and Materials Engineering, College of Engineering, University of Tehran, Iran.*
[c] *Professor, Department of Materials Science & Engineering, Faculty of Technology and Engineering, Imam Khomeini International University (IKIU), Qazvin, Iran.*
[d] *Assistant Professor, Department of Chemical and Materials Engineering, Buein Zahra Technical University (BZTE), Buein Zahra, Qazvin, Iran.*
* Corresponding author Email: m.rajabi@eng.ikiu.ac.ir (M. Rajabi) URL: https://www.acerp.ir/article_241350.html

ARTICLE INFO

Article History:
Received 07 June 2025
Received in revised form 17 November 2025
Accepted 21 December 2025

Keywords:
Ti6Al4V,
Diamond-like Carbon,
TiCN,
Coating,
PACVD,
Wear

ABSTRACT

In this investigation, gradient interlayers of diamond-like carbon (DLC) and titanium carbonitride (TiCN) were applied to a titanium-based alloy (Ti6Al4V) using the PACVD (plasma-assisted chemical vapor deposition) technique to enhance its performance characteristics. The TiCN interlayer played a crucial role in increasing hardness, elastic modulus (Er), and interfacial bonding strength. Extending the TiCN deposition duration from 2 to 3 hours led to improved DLC adhesion and resulted in a nanocomposite coating thickness of ~1 µm. Mechanical properties were assessed through nanoindentation, hardness measurements, and adhesion evaluations, while tribological behavior was examined via pin-on-disk (POD) wear testing. Surface morphology and wear mechanisms were characterized using field emission scanning electron microscopy (FESEM), optical microscopy (OM), X-ray diffraction (XRD), and Raman spectroscopy. The coated Ti6Al4V substrate demonstrated reduced indentation depth (192 nm), hardness values ranging from 3.8 to 4.7 GPa, and a broader distribution of elastic modulus (136–171 GPa). Frictional behavior of the coated samples showed fluctuating coefficients of friction (µ), attributed to the multilayer structure, whereas the uncoated substrate maintained a relatively stable µ around 0.23. Wear rate analysis revealed that the uncoated alloy exhibited a significantly higher average wear rate (8.1×10^{-7} cm³/N·m) compared to the TiCN/DLC-coated variant (4.1×10^{-8} cm³/N·m). Microscopic examination indicated that the coated surface predominantly experienced adhesive wear, while the uncoated surface was subject to abrasive wear mechanisms.

https://doi.org/10.30501/acp.2026.528459.1178

1. INTRODUCTION

Ti6Al4V, commonly referred to as the Ti64 alloy, contains 6 wt% aluminum and 4 wt% vanadium. Its mechanical properties are strongly influenced by its microstructure, which is determined by both its chemical composition and thermomechanical processing parameters (Baltatu et al. 2020). Ti64 is categorized as a dual-phase titanium alloy, comprising alpha (α-HCP) and beta (β-BCC) phases (Chand et al. 2025). Due to its exceptional thermal stability, mechanical strength, formability, weldability, high specific strength, corrosion resistance, and outstanding biocompatibility, this alloy finds extensive applications in the medical, chemical, automotive, and energy sectors. These applications have led to the development of the Ti64 alloy, which constitutes 60% of the total titanium production (Chen et al. 2011, Elmkhah et al. 2020, Poondla et al. 2009). Although the Ti64 alloy possesses exceptional

Please cite this article as: Newpour, A., Kazemi, M., Rajabi, M. & Ghorbani, H. (2025). Mechanical and Tribological Properties of Ti-6Al-4V by Deposition of Multilayered Coating with PACVD Technique, *Advanced Ceramics Progress*, 11(2), 42-49. https://doi.org/10.30501/acp.2026.528459.1178

properties, its application in biomedical devices such as hip and knee joint prostheses, heart valve replacements, and dental implants is limited by its inherently low surface hardness and suboptimal wear resistance (Yang et al. 2016). These shortcomings are primarily attributed to the alloy's low thermal conductivity and coefficient of friction (μ), which promote the generation of wear debris in the implant region, potentially leading to tissue irritation and cytotoxic effects (Qin et al. 2018). Over the past decade, there has been a marked increase in research focused on surface modification techniques for titanium-based biomaterials, aiming to enhance the surface performance of Ti64 alloys (Ghadai et al. 2021). Among them, TiCN films are considered advanced engineering materials due to their outstanding hardness, robust corrosion resistance, satisfactory thermal and electrical conductivity, and excellent biocompatibility (Gül et al. 2021, Lu et al. 2025). The covalent bonding structure of TiCN contributes significantly to its superior wear resistance (Hung et al. 2013, Zhang et al. 2019).

DLC is a metastable version of amorphous hydrogenated carbon. DLC thin films are among the industrial coatings with high hardness and low μ, which refers to unstable amorphous carbon with a relatively high percentage of SP^3 bonds in its structure (Kang et al. 2015, Samiee et al. 2024). The significant residual stress in the lattice structure is typically responsible for the DLC coatings' great hardness (Khodayari et al. 2023). DLC-based coatings have significant potential for use as coating materials in the biomedical industry due to their high hardness and outstanding biocompatibility. The performance of biocompatible compounds and alloys coated with DLC has been reported in significant numbers (Kumar et al. 2024, and Liu et al. 2004). The quality of DLC coatings is closely associated with the deposition factors (voltage, current, power supply, working pressure, and precursor type), the substance used, and the energy of the ions engaged in chemical processes that determine the proportions of hydrogen and carbon linked in chains and graphite rings. For coating titanium-based alloys, chemical vapor deposition (CVD) (Rajak et al. 2021), atmospheric pressure CVD (APCVD) (Elmakhah et al. 2020), sol-gel (Rajak et al. 2021), thermal spraying (Wu et al. 2024), plasma-assisted CVD (PACVD) (Khodadyari et al. 2023), and physical vapor deposition or PVD are some of the most significant conventional methods (Wu et al. 2024, Movassagh Alanagh et al. 2017). The PACVD method is the most accessible and convenient way to overcome the issues present in other methods. This method is the main process for synthesizing medical biocompatibility components, and it has recently been used for altering the mechanical and tribological properties of titanium-based alloys (Khodadyari et al. 2023).

Three films, including TiN, TiCN, and Ti-DLC, were deposited and coated on 316L stainless steel. The TiCN film had the greatest hardness and elastic modulus among them, followed by the Ti-DLC and lastly the TiN (Rahmati et al. 2016). Movassagh Alanagh et al. (2018) used the pulsed-DC PACVD to explore the titanium silicon nitride (TiSiN) ceramic coating on the Ti64 alloy. The results showed that the creation of SiO_2 and TiO_2 coatings on the Ti64 alloy's surface increased its corrosion resistance. Additionally, coatings with 2.17 wt% and 3.11 wt% Si were shown to have the highest wear resistance (Movassagh Alanagh et al. 2025).

Hang et al. (2013) successfully used the pulsed-DC PACVD technology to coat hydroxyapatite (HA) on dental implants with a 4.5 mm diameter. According to the microscopic images, the HA coating surface was roughly consistent in thickness, measuring between 130 and 147 mm. Using the FVA technique, Kang et al. (2015) set a TiCN interlayer between the DLC film and the Ti64 alloy after depositing a DLC film. The resultant μ of the TiCN interlayer on the DLC-coated Ti64 was a minuscule 0.03.

This study aims to enhance the mechanical and tribological performance of Ti64 alloy by applying gradient TiCN/DLC coatings using the PACVD method. The investigation focuses on evaluating the effects of varying deposition parameters on coating adhesion, hardness, elastic modulus, and wear behavior. In this research, the primary method for improving the surface properties of the Ti64 alloy is to apply a layer with high hardness and low μ to achieve desirable adhesion, corrosion resistance, and biocompatibility. The primary surface reinforcement coating for this application was DLC, while the intermediate layer was TiCN. Hardness, POD wear, and wettability tests were utilized to assess the mechanical, tribological, and corrosion characteristics of the coatings that were created. FESEM, OM, XRD, and Raman spectroscopy were utilized to investigate the samples' surfaces and wear mechanisms.

2. MATERIALS AND METHODS

2.1. Sample preparation

A Ti64 specimen with dimensions of 10 mm × 10 mm × 10 mm was prepared using wire electrical discharge machining. To eliminate surface oxides and contaminants, the substrate was mechanically polished using silicon carbide (SiC) sandpapers ranging from #800 to #2000 grit. Subsequent ultrasonic cleaning was performed in acetone and deionized water. The cleaned substrates were then mounted onto the substrate holder for coating procedures. All deposition processes were conducted using a pulsed-DC PACVD, comprising four primary components: a vacuum pump, a power supply, a vacuum chamber, and a gas flow controller. The reaction chamber, a cylindrical vessel with a diameter of 50 cm and a length of 70 cm, operated under a current of 10 A and a pressure range of 0.2-0.4 mbar. Temperature regulation was achieved via a thermocouple and external heaters. Before coating, surface impurities were further removed through ion bombardment under argon gas for one hour. To enhance the adhesion of the coating to the

Ti64 substrate, plasma nitridation was carried out at 450 °C for 3 hours. TABLE 1 summarizes the experimental parameters used during the deposition of the TiCN interlayer under a mixed gas atmosphere of H_2, N_2, and CH_4.

After nitridation and deposition, a TiCN gradient interlayer coating was formed on Ti64 over periods of 2 and 3 h. For the deposition of the DLC coating, the sample is first cleaned with acetone and placed on the cathode. The plasma process was formed by establishing a potential difference between the cathode and anode at a chamber temperature of 150℃. The potential between the cathode and anode was cut off after the coating of the samples was completed, and finally, after preventing gas from entering the chamber and cooling the samples to room temperature, the samples were removed from the chamber.

2.2. Surface and structural characterization

The surface topographical and microstructure of the specimens were studied with the FESEM model S360-MV2300. To characterize the phases in coating structures, a Philips XRD apparatus with an $\alpha = 2°$, step size = 0.03° incidence angle, and Cu-Kα radiation ($\lambda = 1.54$ Å) was utilized. To enhance image contrast and analyze coatings, samples were etched for 5 minutes with deionized water and 70% nitric acid (HNO3) solution. A Raman spectrometer was used to identify bond types in the DLC coating at a wavelength of 523 nm, power is 30 mW, a resolution is 4 cm^{-1}, and the model is the P50C0R10.

2.3. Mechanical and tribological characteristics

The adhesion performance of the coatings applied to the Ti64 was evaluated in accordance with the VDI 3198 standard using the Rockwell-C indentation method. A load of 150 kg was applied to the coated surfaces, and the resulting indentation patterns were analyzed to determine the coating-substrate adhesion quality. OM was employed to further assess the extent and nature of coating delamination or cracking around the indentations. To characterize the mechanical properties of the coatings, nanoindentation testing was conducted to measure the E_r and hardness. This technique involves recording the force-displacement response of a precision indenter as it penetrates the sample surface over time, reflecting the mechanical response of the material. A nanoindentation system with a resolution of 10^{-9} was utilized, and the resulting load-depth curves were analyzed using Hystron TriboScope software to extract quantitative values of hardness and elastic modulus. The tribological behavior of the coated and uncoated samples was examined using a POD tribometer, following the ASTM G99 standard. Parameters such as the coefficient of friction (μ) and specific wear rate were measured to evaluate wear resistance. The POD tests were performed under controlled conditions: a normal load of 40 N, a sliding distance of 600 m, a track radius of 13 mm, and a sliding speed of 0.4 cm/s. These tests provided insights into the wear mechanisms and durability of the coatings under simulated service conditions.

3. RESULT AND DISCUSSION

3.1. Surface and structural characterization

Figure 1 shows FESEM images of the DLC coating on the Ti64 substrate obtained using the PACVD process. The bright areas in Figure 1 (a) and (b) demonstrate the carbon present in the coated layer, where the layer formation process has not been fully completed, and the corresponding hybridization bonds have not formed. In this case, the carbon formed on the surface acts as an electrical insulator, creating a bright contrast in microscopic images. Based on the FESEM images, the presence of bright regions on the surface of the DLC coating indicates areas where the deposition process was incomplete. These regions suggest that the carbon atoms did not undergo sufficient hybridization to form stable sp^2 or sp^3 bonds, which are characteristic of well-structured DLC films. The lack of proper bonding may result from suboptimal PACVD parameters such as insufficient plasma density, inadequate substrate temperature, or non-uniform precursor distribution during deposition. Consequently, the carbon in these zones remains in a disordered, amorphous state and behaves as an electrical insulator, leading to the observed bright contrast in SEM micrographs. The duration of the TiCN interlayer coating affects the adhesion of the DLC coating on it. After 2 h of deposition, it was observed that the DLC coating did not adhere well to the TiCN layer in some areas, and the carbon deposition was not satisfactory.

This issue led to the formation of non-conductive carbon on the surface of the coating, creating bright contrasts in the images. With a slight modification and an increase in the coating duration of the TiCN interlayer from 2 to 3 h, it was observed that the adhesion of the DLC coating on this interlayer improved, and the layer thickness increased from the range of ~1 μm, becoming more homogeneous. Figure 2 shows the surface and cross-section images of the coated specimens after 2 and 3 h of deposition.

TABLE 1. The conditions of the experimental variables during deposition.

Coating	Frequency (KHz)	Flow (A)	Voltage (V)	Temperature (℃)	Time (min)	Flow rate (sccm)
TiN	50	2-3	450	450-500	180	N_2:50, H_2:200
TiCN	50	2-3	450	500	60	N_2:50, H_2:300
DLC	50	2-3	450	150	120	Ar:50, CH_4:6

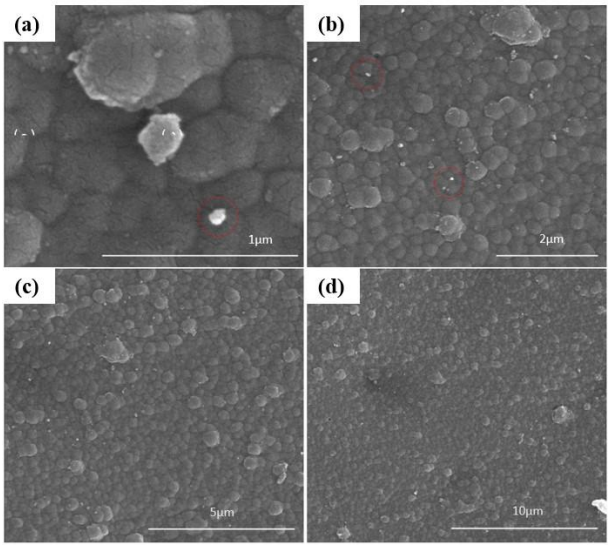

Figure 1. (a-d) FESEM images of the DLC coating on the substrate using the PACVD.

Figure 3 depicts the XRD pattern of a thin layer from two samples: a silicon wafer coated with DLC and a Ti64 alloy sample. The DLC coating was first applied to the silicon wafer using the PACVD technique. A phase analysis was then carried out to look at the phases that formed on the coating's surface. Considering the distinct diffraction peaks corresponding to single-crystal silicon, the precise peaks resulting from the coating can be determined. Graphite, diamond, and silicon carbide (SiC) phases are identified as the peaks. With this interpretation and the re-analysis of the DLC/TiCN coating on the Ti64 substrate, it was observed that there are no signs of potential graphite and diamond phases in the characteristic peaks.

The lack of detection or formation of such peaks may be attributed to various factors, including the small amount of formed phases and differences in the phase structure in terms of growth morphology on the two different substrates.

Figure 4 shows the Raman spectroscopy for the DLC coating using a TiCN interlayer on a Ti64 substrate. The presence of F and H peaks indicates the formation of graphite nanocrystals. The peak corresponding to the H band indicates the vibrations of carbon atoms with Sp^2 hybridization in carbon rings and chains (C-C) with a wavenumber of 1594 cm^{-1} and an intensity of 3192. The peak corresponding to band F also indicates the vibrations of carbon atoms with Sp^2 hybridization in aromatic hexagonal rings with a wavenumber of 1373 cm^{-1} and an intensity of 2682. The wavenumber values deviate from the ideal state, which may be due to residual stresses induced by the coating.

In fact, thermal stresses are generated during the deposition of DLC/TiCN coatings on the substrate, which is indicative of the difference in thermal expansion coefficients between the Ti64 substrate (8.6 W/m.k) and the DLC/TiCN coatings (0.8 W/m.k).

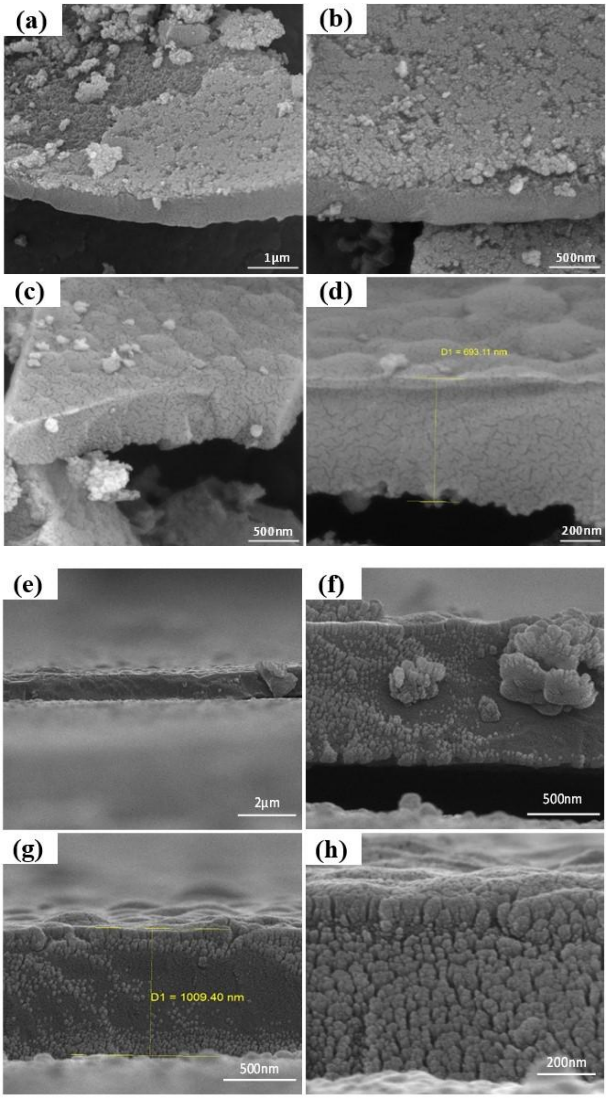

Figure 2. FESEM micrographs of the DLC layer deposited on the Ti64 substrate via PACVD, shown for deposition durations of (a-d) 2 hours and (e-h) 3 hours.

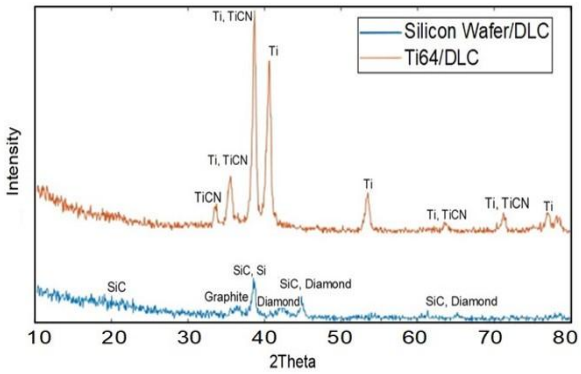

Figure 3. XRD spectra of thin-film specimens, including Ti64 and silicon wafers coated with DLC.

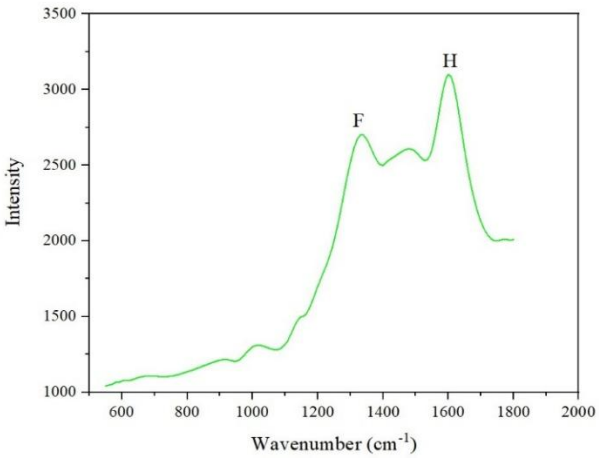

Figure 4. Raman spectrum of the DLC/TiCN coating deposited on the Ti64 substrate by PACVD.

3.2. Mechanical And Tribological Behavior

Figure 5 shows the typical effects of Rockwell-C hardness testing. Hardness testing was conducted on coatings with 2 and 3 h TiCN interlayer deposition times. Interlayer coatings with a deposition time of 3 h have better adhesion quality.

The differences in plastic deformation and shear stress created are due to the deposition time of the TiCN interlayer and consequently affect the thickness and uniformity of the coating. Increasing the coating thickness may help reduce stress concentration on the substrate surface and absorb the energy resulting from the applied load. On the other hand, the uniformity of the coating leads to an even distribution of stresses on the substrate surface and prevents stress concentration at specific points and more severe plastic deformation.

Thicker and more homogeneous coatings usually increase surface hardness, which can improve resistance to plastic deformation. The coating deposited for 2 h exhibited poor adhesion to the TiCN interlayer, which resulted in severe plastic deformation and delamination during indentation, as clearly observed in Figure 5 (c,d). These defects correspond to the HF5 fracture pattern, indicating that the coating was unable to withstand the applied stresses and failed prematurely.

The weak bonding between the DLC layer and the underlying substrate, combined with insufficient coating thickness, contributed to the propagation of cracks and the detachment of the film under mechanical loading.

In contrast, the coating deposited for 3 h demonstrated a markedly improved adhesion and mechanical integrity. As shown in Figure 5 (a,b), the indentation response followed the acceptable HF3 failure pattern, which is characteristic of a stable film capable of resisting shear stresses without catastrophic delamination.

The increased deposition time led to a thicker and more homogeneous DLC layer, enhancing the interfacial bonding with the TiCN interlayer. This improvement reduced the tendency for crack initiation and propagation, thereby allowing the coating to accommodate the applied load more effectively. The transition from HF5 to HF3.

According to Figure 2 all deformations occurred within the coated area, and the substrate did not affect the obtained results.

By comparing the effect of coating, it was observed that the lack of coating on the alloy led to an increase in indentation at a fixed force, which directly affects their hardness and elastic modulus. The area within each hysteresis loop created indicates the amount of energy wasted on the surface due to plastic deformation. An increase in indentation referred to the larger penetration depth and more severe deformation observed in the 2 h coated sample during the indentation test. This behavior is associated with poor adhesion and delamination, as shown in Figure 5 (c,d), and corresponds to the HF5 failure pattern.

In contrast, the 3 h coated sample exhibited reduced indentation depth and a more stable response, following the acceptable HF3 failure pattern (Figure 5 (a,b)). Therefore, the 3 h coating demonstrates improved mechanical properties and adhesion compared to the 2 h coating.

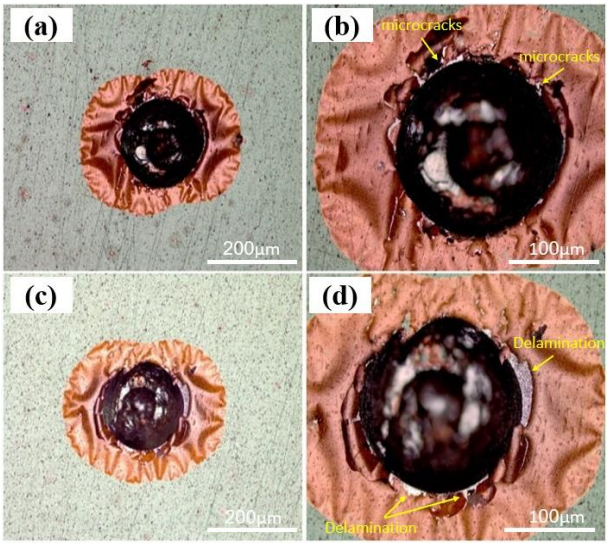

Figure 5. Representative results of Rockwell-C hardness testing after (a–b) 3 hours and (c–d) 2 hours.

Figure 6 illustrates the relationship between E_r and hardness with respect to maximum indentation depth for both uncoated and TiCN/DLC-coated Ti64 substrates. As expected, both parameters tend to decrease with increasing indentation depth.

These values are derived from the unloading segment of the nanoindentation force-displacement curves. Comparative analysis reveals that the uncoated substrate exhibits greater indentation depths, corresponding to lower hardness (2.2–4.5 GPa) and E_r (57–67 GPa) values.

In contrast, the coated samples demonstrate improved mechanical performance, with hardness ranging from 3.8 to 4.7 GPa and Er values between 136 and 171 GPa.

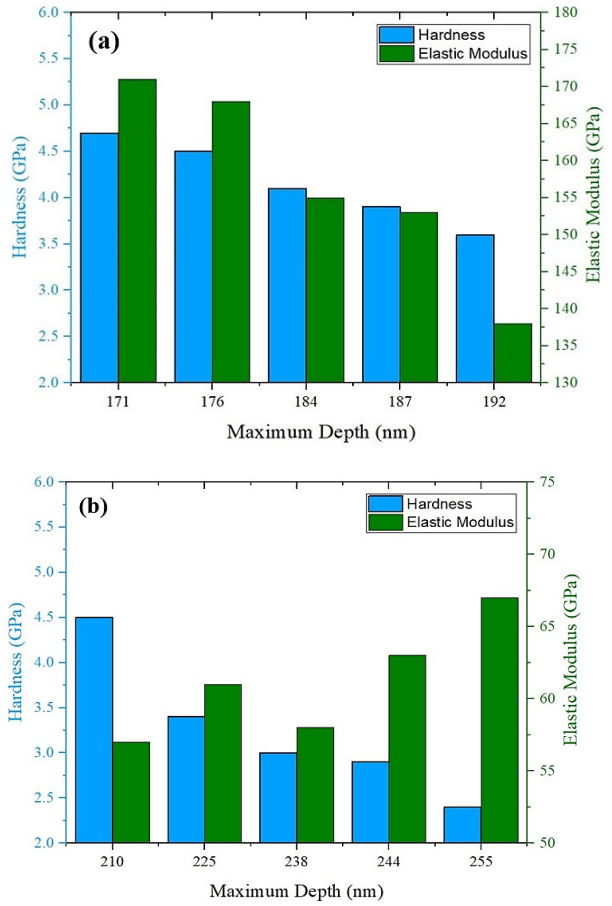

Figure 6. Hardness and E_r curves as a function of maximum depth for Ti64 substrate (a) with TiCN/DLC coating and (b) without coating.

The variation in the μ as a function of sliding distance for the Ti64 substrate, both with and without coating, is illustrated in Figure 7. For the uncoated substrate, μ remains relatively stable throughout the test, maintaining an average value around 0.23.

This consistency suggests minimal change in surface interaction over the sliding distance. In contrast, the coated sample exhibits a dynamic behavior. Initially, over the first 60 m of sliding, the μ gradually increases. This rise indicates progressive wear of the outermost coating layer, eventually exposing the underlying TiCN interlayer and the substrate itself.

As the coating deteriorates, the tribological interface evolves, leading to changes in frictional response. Beyond this point, μ begins to decrease due to mechanical oscillations introduced by the steel pin used in the test setup. These oscillations are associated with the repositioning and stabilization of the pin on the DLC-coated surface.

The fluctuations persist until approximately 250 m of sliding distance, at which point the pin achieves a stable contact with the sample. Once stabilized, the coefficient of friction for the DLC coating settles at a lower value, approximately 0.12, reflecting the lubricious nature of the DLC layer. To evaluate and compare the wear performance of the coated and uncoated samples, the Archard wear law is employed.

This empirical model establishes that the specific wear rate is directly proportional to the applied normal load and the total sliding distance, and inversely proportional to the material hardness. By applying this law, one can quantitatively assess the wear resistance of each configuration and better understand the protective effect of the coating under tribological stress.

The Archard equation, expressed as $K=\frac{V}{F\cdot S}$ quantifies the specific wear rate (K) by relating the wear volume (V) to the product of the applied contact force (F) and the sliding distance (S), thereby describing the reduction in material volume due to wear.

The results show that the average K of uncoated samples (8.7×10^{-7} cm^3/N.m) is higher than that of coated samples ($4.1\times10^{-8}$$cm^3$/N.m). The DLC coating has high hardness and low friction coefficient (Wu et al. 2024). The lower wear rate of the coated samples is likely due to their increased wear resistance and lower friction.

Figure 8 shows the OM images for investigating wear mechanisms. Due to wear on the Ti64 substrate, scratches were formed on the surface of the substrate. The grooves resulting from the wear indicate an abrasive wear mechanism.

In the coated sample parts of the worn surface have detached due to the weakening of the adhesion of DLC on the TiCN interlayer, resulting in delamination on the coating surface.

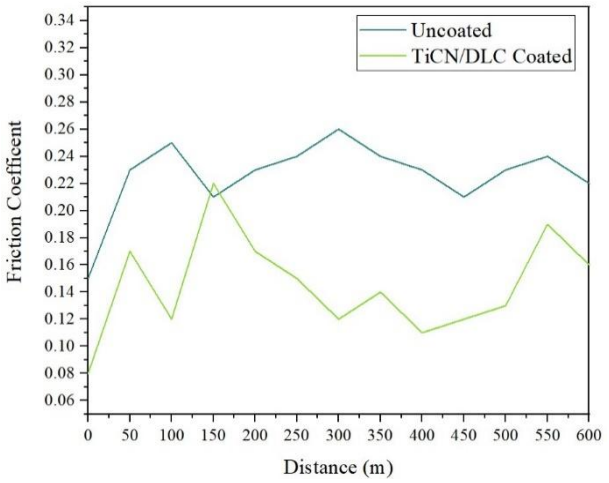

Figure 7. Hardness and E_r curves as a function of maximum depth for Ti64 substrate (a) with TiCN/DLC coating and (b) without coating.

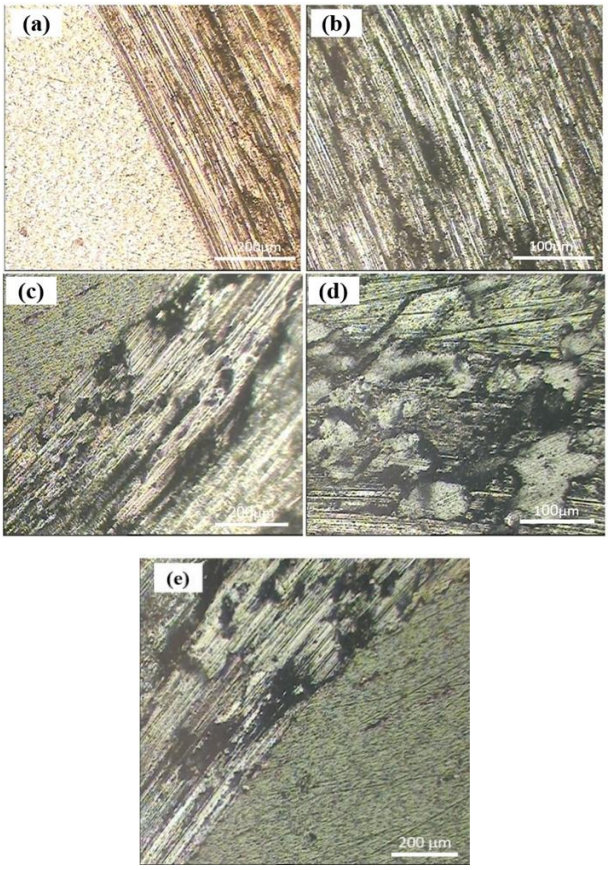

Figure 8. OM images resulting from POD on the substrate (a), (b) without coating, and (c-e) with TiCN/DLC coating.

4. CONCLUSION

In this study, DLC was deposited as the main reinforcing coating and TiCN as an intermediate layer on the Ti64 alloy using pulsed-DC PACVD. The Raman spectroscopy results of the samples indicate the formation of nano-graphite crystals, and the deviation of the peaks from the ideal state is due to the residual stress created by the TiCN/DCL coating.

With the increase in the coating duration of the TiCN interlayer from 2 to 3 h, it was observed that the adhesion of DLC on the interlayer improved, and the layer thickness increased from ~693 to ~1009 nm, becoming more homogeneous.

Microscopic images obtained from Rockwell-C hardness testing effects showed that increasing the coating thickness of samples enhanced the hardness, improving resistance to plastic deformation.

By comparing the coating effect for the Ti64 substrate with and without the TiCN/DLC coating, it was reported that the indentation depth due to coating decreased from 258 to 192nm. Additionally, the hardness and E_r values of the uncoated substrate were obtained in the ranges of 2.5-4.2 and 57-67 GPa, respectively, both of which are lower than those of the coated substrate, which had hardness and E_r values in the ranges of 3.8-4.7 and 136-171 GPa.

Tribological studies of the samples showed that the μ of the uncoated substrate is in a nearly constant range of 0.23, but for the coated substrate, there are upward and downward fluctuations in μ due to the different hardness of the coatings. The experiment found that uncoated samples have a higher average wear rate (8.7×10^{-7} cm^3/N.m) than coated samples (4.1×10^{-8} cm^3/N.m). OM images show that the wear mechanism for the uncoated substrate is abrasive, while for the coated substrate, it is adhesive.

ACHNOWLEDGMENT

The authors gratefully acknowledge Imam Khomeini International University (IKIU) for providing financial support for this work.

REFERENCES

1. Baltatu, M. S., Vizureanu, P., Sandu, A. V., Munteanu, C., & Istrate, B. (2020). Microstructural analysis and tribological behavior of Ti-based alloys with a ceramic layer using the thermal spray method. *Coatings*, *10*(12), 1216. https://doi.org/10.3390/coatings10121216

2. Chand, N., et al. (2025). Diamond-like carbon (DLC) coating on TZM alloy for enhanced performance in high-temperature applications. *J. Alloys Compd. Commun.*, *6*, 100077. https://doi.org/10.1016/j.jacomc.2025.100077

3. Chen, R., Tu, J., Liu, D., Mai, Y., & Gu, C. (2011). Microstructure, mechanical, and tribological properties of TiCN nanocomposite films deposited by DC magnetron sputtering. *Surf. Coat. Technol.*, *205*(21-22), 5228–5234. https://doi.org/10.1016/j.surfcoat.2011.05.034

4. Elmkhah, H., Fattah-alhosseini, A., Babaei, K., Abdollah-Zadeh, A., & Mahboubi, F. (2020). Correlation between the Al content and corrosion resistance of TiAlN coatings applied using a PACVD technique. *J. Asian Ceram. Soc.*, *8*(1), 72-80. https://doi.org/10.1080/21870764.2019.1709274

5. Ghadai, R., Das, S., Kalita, K., Swain, B., & Davim, J. P. (2021). Structural and mechanical analysis of APCVD deposited diamond-like carbon thin films. *Silicon*, *13*(12), 4453-4462. https://doi.org/10.1007/s12633-020-00760-3

6. Gül, C., Albayrak, S., Durmuş, H., & Çömez, N. (2021). Characterization of SiO_2 sol-gel coated Ti6Al4V alloy obtained by using TEOS and GPTMS. *Sci. Sinter.*, *53*(4), 461. https://doi.org/10.1016/j.matpr.2020.11.1023

7. Hung, K. Y., Shih, P. Y., Yang, Y. C., Feng, S. W., & Lin, C. T. (2013). Titanium surface modified by hydroxyapatite coating for dental implants. *Surf. Coat. Technol.*, *231*, 337-345. https://doi.org/10.1016/j.surfcoat.2012.03.037

8. Kang, S., Lim, H. P., & Lee, K. (2015). Effects of TiCN interlayer on bonding characteristics and mechanical properties of DLC-coated Ti-6Al-4V ELI alloy. *Int. J. Refract. Met. Hard Mater.*, *53*, 13-16. https://doi.org/10.1016/j.ijrmhm.2015.04.028

9. Khodayari, A., Elmkhah, H., Alizadeh, M., & Maghsoudipour, A. (2023). Modified diamond-like carbon (Cr-DLC) coating applied by PACVD-CAPVD hybrid method: Characterization and evaluation of tribological and corrosion behavior. *Diamond Relat. Mater.*, *136*, 109968. https://doi.org/10.1016/j.diamond.2023.109968

10. Kumar, A., & Singh, G. (2024). Surface modification of Ti6Al4V alloy via advanced coatings: Mechanical, tribological, corrosion, wetting, and biocompatibility studies. *J. Alloys Compd.*, 174418. https://doi.org/10.1016/j.jallcom.2024.174418

11. Liu, X., Chu, P. K., & Ding, C. (2004). Surface modification of titanium, titanium alloys, and related materials for biomedical applications. *Mater. Sci. Eng. R Rep.*, *47*(3-4), 49-121. https://doi.org/10.1016/j.mser.2004.11.001

12. Lu, F., Ma, Q., Liu, E., Wei, R., Bai, J., Gao, Q., & Qi, J. (2025). Advancements in understanding the microstructure and properties of additive manufacturing Ti-6Al-4V alloy: A comprehensive review. *Journal of Alloys and Compounds*, 180543. https://doi.org/10.1016/j.jallcom.2025.180543

13. Movassagh-Alanagh, F., Abdollah-Zadeh, A., & Aghababaei, R. (2025). Effects of B and C elements on microstructure, mechanical, and tribological properties of TiN coating deposited by PACVD. *Mater. Charact.*, 115178. https://doi.org/10.1016/j.matchar.2025.115178

14. Movassagh-Alanagh, F., Abdollah-Zadeh, A., Aliofkhazraei, M., & Abedi, M. (2017). Improving the wear and corrosion resistance of Ti-6Al-4V alloy by deposition of TiSiN nanocomposite coating with pulsed-DC PACVD. *Wear*, *390*, 93-103. https://doi.org/10.1016/j.wear.2017.07.009

15. Movassagh-Alanagh, F., Abdollah-Zadeh, A., Asgari, M., & Ghaffari, M. A. (2018). Influence of Si content on the wettability and corrosion resistance of nanocomposite TiSiN films deposited by pulsed-DC PACVD. *J. Alloys Compd.*, *739*, 780-792. https://doi.org/10.1016/j.jallcom.2017.12.235

16. Poondla, N., Srivatsan, T. S., Patnaik, A., & Petraroli, M. (2009). A study of the microstructure and hardness of two titanium alloys: Commercially pure and Ti-6Al-4V. *J. Alloys Compd.*, *486*(1-2), 162-167. https://doi.org/10.1016/j.jallcom.2009.06.172

17. Qin, Y., Zheng, G., Zhu, L., He, J., Zhang, F., Dong, Y., & Yin, F. (2018). Structure and wear characteristics of TiCN nanocomposite coatings fabricated by reactive plasma spraying. *Surface and Coatings Technology*, *342*, 137-145. https://doi.org/10.1016/j.surfcoat.2018.02.108

18. Rahmati, B., Sarhan, A. A., Basirun, W. J., & Abas, W. A. B. W. (2016). Ceramic tantalum oxide thin film coating to enhance the corrosion and wear characteristics of Ti6Al4V alloy. *J. Alloys Compd.*, *676*, 369-376. https://doi.org/10.1016/j.jallcom.2016.03.188

19. Rajak, D. K., Kumar, A., Behera, A., & Menezes, P. L. (2021). Diamond-like carbon (DLC) coatings: Classification, properties, and applications. *Appl. Sci.*, *11*(10), 4445. https://doi.org/10.3390/app11104445

20. Samiee, M., Seyedraoufi, Z. S., Abbasi, M., Eshraghi, M. J., & Abouei, V. (2024). Diamond-like carbon (DLC) coating on graphite: Investigating the achievement of maximum wear properties using the PECVD method. *Ceram. Int.*, *50*(12), 21439-21450. https://doi.org/10.1016/j.ceramint.2024.03.255

21. Wu, Z., Liu, R., Liu, Z., Wu, X., & Li, F. (2024). Microstructure and properties of multilayer TiN/TiCN nanocrystalline coating used for a metal bipolar plate. *Vacuum*, *227*, 113361. https://doi.org/10.1016/j.vacuum.2024.113361

22. Yang, D., & Liu, Z. (2016). Quantification of microstructural features and prediction of mechanical properties of a dual-phase Ti-6Al-4V alloy. *Materials*, *9*(8), 628. https://doi.org/10.3390/ma9080628

23. Zhang, J., Lou, J., He, H., & Xie, Y. (2019). Comparative investigation on the tribological performances of TiN, TiCN, and Ti-DLC film-coated stainless steel. *JOM*, *71*, 4872-4879. https://doi.org/10.1007/s11837-019-03718-y